Copper–1,10-Phenanthroline Complexes Binding to DNA: Structural Predictions from Molecular Simulations

ARTICLE *in* THE JOURNAL OF PHYSICAL CHEMISTRY B · SEPTEMBER 2009

Impact Factor: 3.3 · DOI: 10.1021/jp901210g · Source: PubMed

Copper−1,10-Phenanthroline Complexes Binding to DNA: Structural Predictions from Molecular Simulations

Arturo Robertazzi,[†,‡,§] Attilio Vittorio Vargiu,[†,‡,§] Alessandra Magistrato,[*,†,∥] Paolo Ruggerone,[‡] Paolo Carloni,[†,∥,⊥] Paul de Hoog,[#] and Jan Reedijk[#]

SISSA, via Beirut 4, I-0 I-34014 Trieste, Italy, CNR-INFM SLACS and Dipartimento di Fisica, Università di Cagliari, S.P. Monserrato-Sestu Km 0.700, I-09042 Monserrato, Italy, CNR-INFM-DEMOCRITOS National Simulation Center, Via Beirut 4, I-34014 Trieste, Italy, Italian Institute of Technology − SISSA unit, Via Beirut 4, I-34014 Trieste, Italy, and Leiden Institute of Chemistry, Gorlaeus Laboratories, Leiden University, P.O. Box 9502, 2300 RA Leiden, The Netherlands

Received: February 10, 2009; Revised Manuscript Received: May 29, 2009

Copper−1,10-phenanthroline (phen) complexes $Cu(phen)_2$, Cu(2-Clip-phen), and Cu(3-Clip-phen) (Clip = a serinol bridge between the phen parts) are typically employed as DNA-cleaving agents and are now becoming increasingly important for building multifunctional drugs with improved cytotoxic properties. For instance, Cu(3-Clip-phen) has been combined with distamycin-like minor-groove binders and cisplatin-derivatives, leading to promising results. Density Functional Theory (DFT) and docking calculations as well as molecular dynamics (MD) simulations were performed to describe the mode of binding to DNA of these complexes. Our data suggest the minor-groove binding to be more probable than (partial) intercalation and major-groove binding. In addition, it was found that a combination of factors including planarity, van der Waals interactions with DNA, and structural complementarities may be the key for the cleavage efficiency of these copper complexes.

Introduction

In the last decades, an increasingly number of compounds containing transition metal ions such as platinum and ruthenium have shown to be active against cancer.[1−5] Unfortunately, these drugs have major drawbacks, including poor selectivity toward their biological target (most often DNA) and high toxicity.[6,7] A possible strategy to overcome some of these issues is to combine different drugs in an attempt at improving both efficiency and selectivity of the single components.[8] In this respect, complexes of copper−1,10-phenanthroline (Figure 1) have been recently attached with DNA minor- and major-groove binders,[9−11] leading to increased activity and/or selectivity compared to the single components of the complex.

Copper−1,10-phenanthroline compounds are chemical nucleases whose properties were discovered by Sigman et al. already in 1979 (Figure S1 of the Supporting Information).[12] The potential clinical use[13] of the parent compound $Cu(phen)_2$ [In case the charge is not explicitly mentioned, we refer to the generic complex in both oxidation states.] (Figure 1A) is mainly prevented by two drawbacks: (i) the low binding constant of the second phenanthroline, with consequent formation of Cu(phen), which has remarkably lower cleavage efficiency,[10,14,15] and (ii) the modest sequence selectivity of its DNA cleavage.[16,17] [$Cu(phen)_2^+$ binds DNA triplets according to the following trend: TAT ≫ TGT ≫ CAT, CAC > CGT, CGC; see, for example, refs 16 and 17.]

To address the first issue, a serinol bridge (Clip) was employed that binds together the two aromatic rings on positions 2 or 3, resulting in Cu(2-Clip-phen) and Cu(3-Clip-phen) (Figure 1B−C).[10,14,15] These complexes are 2 and 60 times more efficient than $Cu(phen)_2$, respectively:[10,14,18] the covalent link increases the affinity of the metal for both phenanthroline rings, this being the main reason of the improved efficiency in DNA cleavage. However, it is still not clear why the Cu(3-Clip-phen) complexes show such a robust improvement.[15,19]

In order to improve the modest sequence selectivity of the clipped complexes toward DNA, the amine group of the serinol link was functionalized with sequence specific DNA minor/major-groove binding ligands. Pitié et al. employed a distamycin-like minor-groove binder with both 2-Clip-phen and 3-Clip-phen ligands, the latter resulting in a sequence selective cleaving agent.[20−23] Some of us synthesized hybrid compounds in which a platinum moiety is tethered to Cu(3-Clip-phen).[9] This class of compounds represents an excellent example of a multidrug approach: the platinum unit plays both the role of an antitumor drug and of a sequence selective anchor to the major groove, while the Cu(3-Clip-phen) moiety cleaves the DNA from the minor groove. Such a combination indeed resulted in an improved cytotoxic activity compared to that of cisplatin.[9]

While the mechanism of action of drugs such as cisplatin and distamycin has been extensively investigated (see, for example, refs 2 and 24−30 and references therein), that of copper−1,10-phenanthroline complexes is still matter of debate.[10,31] Many studies led to the conclusion that the reaction of $Cu(phen)_2$ with DNA may occur as follows: (i) the freely diffusing $Cu(phen)_2^{2+}$ is reduced to $Cu(phen)_2^+$, (ii) which binds DNA reversibly; (iii) the noncovalent $Cu(phen)_2^+$/DNA adduct is oxidized by dihydrogen peroxide, forming as yet unknown cleaving species; (iv) these perform an oxidative attack mainly

* Corresponding author.
† SISSA.
‡ Università di Cagliari.
§ Equally contributed to this work
∥ CNR-INFM-DEMOCRITOS National Simulation Center.
⊥ Italian Institute of Technology−SISSA unit.
Leiden University.

10.1021/jp901210g CCC: $40.75
Published on Web 07/09/2009

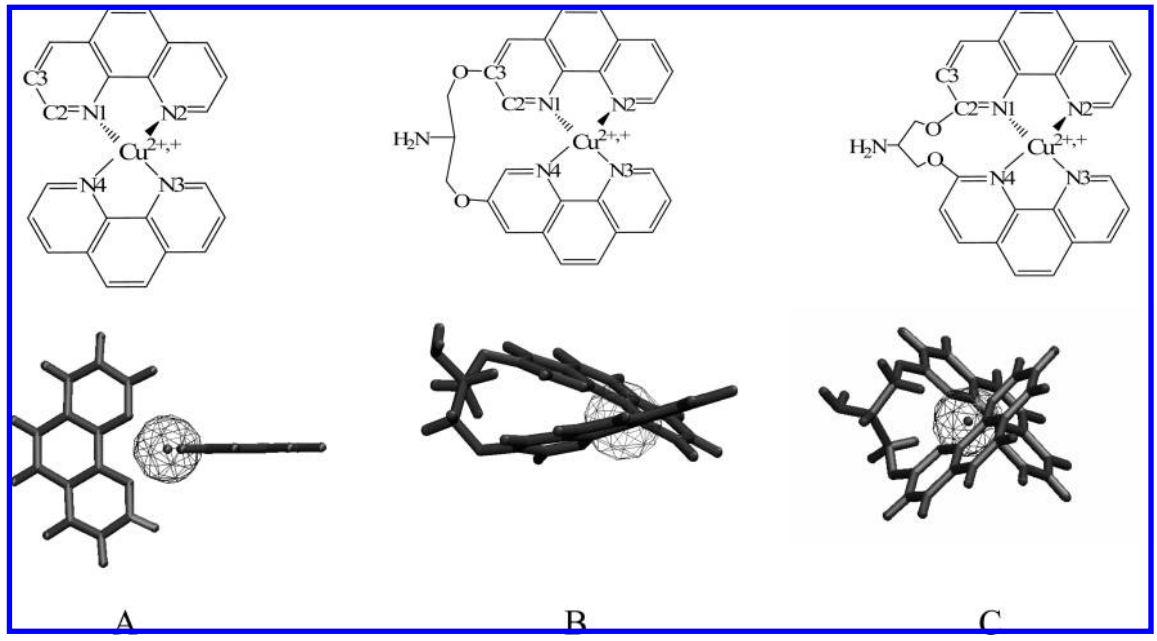

Figure 1. Labeling scheme and DFT[19] optimized structures of (A) $Cu(phen)_2^+$, (B) Cu(3-Clip-phen)$^+$, and (C) Cu(2-Clip-phen)$^+$.

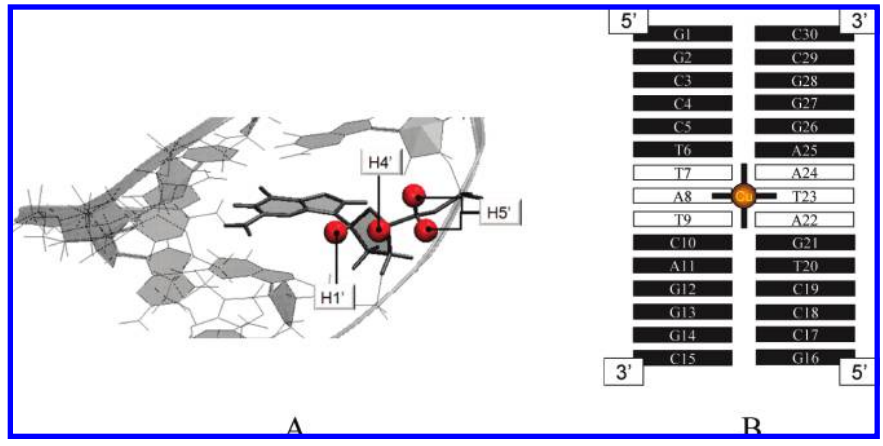

Figure 2. (A) Sugar backbone hydrogen atoms, H1′, H4′, and H5′. C1′ atoms are the carbon atoms of the sugar backbone bound to H1′. (B) Numbering scheme of DNA nucleobases (**TAT** is reported in white).

at C1′, C4′, or C5′ of the 2-deoxyribose units (Figure 2A), eventually leading to DNA cleavage.[21,31−44]

It is further known that cleavage cannot occur when the ligands bind into the major groove, but only when they bind the minor groove.[10,31,45] In particular, two hypotheses (Figure S2 of the Supporting Information) have been proposed for $Cu(phen)_2$ effective binding: (i) one phenanthroline intercalates between two base pairs and the other lies along the minor groove, i.e., partial intercalation,[45] and (ii) one phen ring inside the minor groove, the other partially exposed to the solvent, named simply as minor-groove binding.[10,31] Both models, partial intercalation and minor-groove binding, are compatible with several experimental results.[31,46−51] The DNA-binding mode of clipped complexes is believed to be similar to that of their parent compound.[10]

The partial intercalation hypothesis is consistent with some experiments,[44,52] although no definitive proof has been furnished.[31] The relatively small angle found in the crystallographic structure[53] of $[Cu(phen)_2^+](ClO_4)^-$ between the two phenanthroline rings (N1N2N3N4 ∼50°, see Figure 1 for labeling) may indeed allow intercalation of the complex. However, such a small dihedral angle may primarily be due to crystal packing forces and/or nature of the counterion.[31] Consistently, smaller counterions lead to dihedral angles larger than 70° in the solid state,[31] and NMR studies at room temperature indicate the two phenanthroline ligands to be equivalent,[54] i.e., the angle between the phenanthroline rings is close to 90°.

In contrast, the hypothesis of minor-groove binding is supported by the fact that methyl-substituted copper phenanthroline complexes (Figure S1 of the Supporting Information), which are known to bind the minor groove in a nonintercalative manner,[31] feature an affinity for DNA similar to that of $Cu(phen)_2$.[31] In addition, with the ligand intercalated into DNA, the copper ion would lay inside the minor groove and hence would not be easily accessible to the oxidants.[31] These observations led Sigman to propose a model of minor-groove binding for $Cu(phen)_2$ (Figure S1).[31]

Despite the increasing importance of these compounds as components of potential new anticancer drugs,[9,10] all-atom structural information is not yet available. Experimental structural studies are so far lacking;[10] therefore, a computational approach becomes an important method of choice. However, to the best of our knowledge, the only Molecular Dynamics (MD) simulation study available is on RNA, while no studies have been reported on the interaction with DNA. In particular, Hermann et al.[55] reported ∼1 ns long MD simulation of a

TABLE 1: Selected Structural Parameters (Bonds, Angles, and Dihedral Angles) of Copper Complexes Determined by Several Techniques[a]

	$Cu(phen)_2^+$			$Cu(3\text{-Clip-phen})^+$		$Cu(2\text{-Clip-phen})^+$	
	MD	DFT[b]	exp	MD	DFT[b]	MD	DFT[b]
Cu−N (Å)	2.09 (0.06)	2.08	2.05[b]	2.11 (0.07)	2.10	2.10 (0.08)	2.11
N−Cu−N (deg)	125 (6)	125	130[b]	142 (4)	140	118 (4)	126
N1N2N3N4 (deg)	82 (4)	81	73.0[c], 76.8[c], 49.9[d,e]	44 (4)	49	76 (4)	82

[a] Standard deviations are reported in brackets. [b] Reference 19. [c] Reference 71. [d] Reference 31 and references therein. [e] ClO_4^- as counterion.

$Cu(phen)_2^+$/RNA adduct, suggesting that partial intercalation may be possible in a single-stranded RNA loop. Supported by X-ray data, they also showed that cleavage efficiency may depend on the position of $Cu(phen)_2^+$ inside the RNA, being inversely correlated with the copper distance to the C1′ carbon atoms (Figure 2A).[55] This result confirmed the intuitive idea that the closer the metal center is to the atoms involved in the reaction, the higher the probability of cleavage.

Recent Density Functional Theory (DFT) and docking calculations performed by some of the authors on the three complexes (Figure 1)[19] suggested that the larger activity of Cu(3-Clip-phen) compared to Cu(2-Clip-phen) may be, at least in part, caused by its relatively planar geometry, which allows for a better fit inside the minor groove. More recent DFT studies confirmed that the serinol link mainly affects structural properties rather than electronic ones in complexes similar to those studied here.[56]

In this work, we present a molecular simulation study of the DNA binding of copper−1,10-phenanthroline complexes, which provide structural information of the first step of the DNA cleavage reaction. First, our calculations suggest a rationale for the experimental evidence that cleavage does not occur from the major groove.[31] Second, DFT and steered molecular dynamics (SMD) calculations support the minor-groove binding model.[31] Finally, our data provide insights into the origin of the diverse DNA cleavage efficiency of the three compounds.

Computational Details

Systems. The initial structure of the B-DNA fragment is the 15-mer d(GGCCCT**TAT**CAGGGC)$_2$ (Figure 2B), generated using the nucgen program of the Amber package.[57] This sequence was chosen as copper−1,10-phenanthroline complexes preferentially bind Py-Pu-Py triplets, with **TAT** being the most likely.[16,17] The length of the DNA fragment ensures that end effects will be avoided on the binding mode of the drug (placed close to the center of the fragment). The geometry of copper complexes was taken from our recent studies based on DFT calculations.[19] The initial configurations of the noncovalent copper−1,10-phenanthroline/DNA adducts were built using Autodock,[58] as reported earlier,[19] i.e., confining the search to a central region of six base pairs and containing the **TAT** triplet. Notably, it has been recently reported that Autodock[58] gives good results for complexes binding the DNA.[59]

The total charge of the system was neutralized adding 27 K^+ ions in ∼8000 water molecules for a total of ∼25 000 atoms.

We are aware that the amino group of the clipped complexes may be protonated at physiological pH. Previous studies have indeed suggested that this may be likely for 3-Clip-phen complexes,[15] whereas the amino group of 2-Clip-phen may alternatively coordinate the copper center (this possibly leading to a reduced cleavage efficiency). Thus, not only structural features of the molecules (along with other factors discussed in the Efficiency of Copper−1,10-Phenanthroline Complexes section) but also pH effects may have an influence on the reactivity of these compounds. However, no conclusive experimental evidence has been yet provided about the actual protonation state of these compounds. Thus, for this first contribution, we focus on the structure/function relation and we choose the same protonation state (e.g. neutral) for both 2-Clip-phen and 3-Clip-phen ligands. This in turn allows us to compare the results obtained with this work with our previous DFT studies.[19,56] Further studies, based on both quantum and classical techniques, are required to assess the role of pH effects.

DFT Calculations. DFT calculations were performed using Gaussian03[60] to study the geometry changes of the copper complexes induced by the presence of a counterion. As reported previously,[19] geometry optimizations were carried out without symmetry constraints using the BLYP[50,61] functional, with the 6-31G* basis set on C, H, O, and N atoms and the SDD[62] basis set and ECP on Cu. Harmonic frequency calculations were performed to confirm that calculated structures were minima. To calculate electron densities and estimate solvent effects (with the PCM[63] model as implemented in Gaussian03), single point calculations were performed adding one polarization function on hydrogen and one diffuse function on heavy atoms (6-31+G**). In order to estimate the energetic cost of distortion caused by ClO_4^-, we have defined a strain energy calculated as follows: (i) BLYP/6-31+G** single point on the optimized structure of the ligand, internal energy defined as E_{opt}; (ii) single point on the structure of the ligand optimized with ClO_4^- (this group was then removed for the purpose of calculating the internal energy, E_{ClO4^-}); (iii) the strain energy was finally estimated as $|E_{opt} - E_{ClO4^-}|$.

Parameterization for MD Simulations. The parm99,[64] TIP3P,[65] and Aqvist[66] force fields were used for the DNA duplex, water, and counterions, respectively. Parameters of copper complexes were taken from the Gaff[67] force field with the exception of charges. These were derived from ESP grid points following the Merz−Kollman scheme, and from these a set of RESP atomic charges was derived.[68,69]

Copper parameters for classical MD simulations, $r_{vdW} = 0.96$ Å and $\varepsilon_{well} = 0.01$ kcal/mol, were taken from refs 55 and 70. Missing parameters were built using the parmcal tool of the AMBER[57] package, using the structures obtained from DFT calculations (selected force field parameters were collected in Table S1 of the Supporting Information). Special attention was paid to the dihedral angle between phen rings (N1N2N3N4, Figure 1): a dihedral angle parameter was added for $Cu(phen)_2$ complexes in order to reproduce DFT and experimental structural data (Table 1). A dihedral potential energy function was built as following: DFT single points calculations at different N1N2N3N4 angles were performed to monitor how the internal energy changed; the dihedral potential was then built as reported in the AMBER package manual.[57] In order to check the accuracy of parametrization, ∼3 ns MD simulations for each complex, in solution (and without DNA) were performed, confirming that average structural parameters of the cop-

per−1,10-phenanthroline complexes are close to experimental (if available)[31,71] and DFT[19,56,72,73] data (Table 1).

MD Simulations. Periodic boundary conditions were used, and the electrostatic interactions were calculated with the Particle-Mesh Ewald (PME) method,[74] using a 10 Å cutoff for the real part, as for the van der Waals (vdW) interactions. *NPT* simulations at 300 K and 1 atm were performed using the Nosé−Hoover thermostat[75,76] and the Parrinello−Rahman[77] pressure-coupling scheme. Bonds involving hydrogen atoms were constrained using the lincs algorithm,[78] and a time step of 1.5 fs was used. Translational and rotational motions of the center of mass of the solute were removed every 25 steps.

Geometry optimizations were carried out following a two-step protocol: (i) 10 000 cycles (2000 steepest descent plus 8000 conjugate gradients) with harmonic restraint of $k = 150$ kcal/(mol Å^2) on the solute; (ii) 20 000 conjugate gradients cycles with no restraints. Next, heating up to 300 K was achieved by linearly increasing the temperature in 100 ps of *NVT* MD, while imposing restraints of 50 kcal/(mol Å^2) on the solute. Restraints were then released for 100 ps, and as a last step preceding the productive dynamics, 200 ps of *NPT* MD were carried out. Then, 8 ns for each ligand/DNA adduct as well as for the free DNA in solution were performed. Simulations reached convergence as evidenced by the plots of time evolution of potential energy (see Figure S3 in the Supporting Information displaying the plots of the most relevant adducts as well as free DNA).

Steered molecular dynamics (SMD) simulations[79,80] were performed to investigate Cu(phen)$_2$ partial intercalation. In this method, a force is applied to compel the process of interest to occur on a reasonable time scale for MD simulation. Typically, a molecule (or part of it) is coupled to a dummy point through a spring. This moves toward a given direction, dragging the molecule behind. In this work, the initial direction was defined by the vector from the center of mass of one of the phenanthroline rings and the center of mass of **TA·AT** nucleobases of the **TAT** triplet (Figure S4 of the Supporting Information). The constant-velocity (v) scheme was used in nine different simulations with $v = 0.000\,10$, $0.000\,05$, and $0.000\,01$ Å/time step and force constants (k) of 10, 20, 50 kcal/(mol Å^2). The reliability of this computational approach has been validated by test calculations carried out on a known intercalator for which experimental structure is available (daunomycin, pdb id 1JO2). Results are reported in the Supporting Information.

Calculated Properties. DNA structural parameters were calculated with the program CURVES.[81] The minor-groove width was defined using distances between atoms C4′ of deoxyriboses, subtracted by two carbon atoms van der Waals radii. In order to obtain further information about the way these complexes can bind the DNA, the relative energies of non-bonded interactions, van der Waals and electrostatic (ΔE_{vdW} and ΔE_{el}, respectively), were estimated using the terms of the AMBER force field.[57] Further calculations (see Table S2 of the Supporting Information) were carried out in order to roughly estimate the van der Waals contribution to the binding energy. It is worth stressing that vdW interactions are believed to give the most relevant contribution to the overall binding free energy for most ligands binding noncovalently to the DNA minor groove.[82,83] This is mainly because electrostatic interactions of a free ligand with water molecules and a ligand with DNA are similar, while the hydrophobic effect enhances vdW interactions upon binding. In our specific case, since ΔE_{vdW} is much larger than Δ_{el} (vide infra), the absolute value of $\Delta\Delta_{el}$ is expected to be much smaller than $\Delta\Delta E_{vdW}$.

The vdW contribution to the binding energy was estimated as $\Delta\Delta E_{vdW} = \Delta E_{vdW}^{DNA/solv} + \Delta E_{vdW}^{lig/solv} + \Delta E_{vdW}^{DNA/lig}$, where the first and second terms on the right-hand side of the equation are the change in vdW interaction energy between DNA and solvent and between the ligand and the solvent upon adduct formation; the last term is the vdW interaction energy between the ligand and the DNA in the adduct. Although the standard deviations of $\Delta\Delta E_{vdW}$ are large (particularly due to the large fluctuations of DNA solvation energies), we believe that the trend obtained can qualitatively describe the energetic properties of the studied adducts (vide infra). We would like to stress that the rigorous estimation of interaction free energies is beyond the scope of this work, which is primarily aimed at describing the DNA adducts from a structural point of view.

A cluster analysis was carried out employing the tools of the GROMACS package (using Daura et al.'s algorithm,[84] with an RMSD cutoff of 2 Å),[85−87] in order to identify possible different binding modes of the ligands. For all compounds, a few different conformational clusters of their adducts with DNA were identified; nonetheless, a dominant cluster of conformations was present, containing more than 75% of the sampled configurations. Calculations were carried out using the GROMACS package.[85−87]

Results and Discussion

We report the results of the molecular simulations of the copper(I)−1,10-phenanthroline adducts of DNA fragment d(G-GCCCT**TAT**CAGGGC)$_2$ (hereafter DNA). The major- and minor-groove binding as well as partial intercalation were investigated. Collected structural and energetic data were used to propose a rationale for the experimental DNA cleavage efficiency observed for these complexes.

Major-Groove Binding. Experimental findings established that the major-groove binding mode of copper−1,10-phenanthroline complexes is not relevant for their cleavage activity.[10,31] MD simulations of the three copper(I)−1,10-phenanthroline complexes docked into the DNA major groove were carried out to provide a rationale for this experimental evidence.

During simulation of Cu(phen)$_2^+$/DNA, the ligand progressively detaches from the major groove (Figure S5A of the Supporting Information) and after ∼1 ns, both van der Waals and electrostatic interactions vanish, as complete solvation of the ligand occurs. Similarly, Cu(2-Clip-phen)$^+$ leaves its DNA binding site after ∼4 ns. The longer residence time is most likely due to the serinol−NH_2 group, which forms hydrogen bonds with phosphate oxygen atoms. Cu(3-Clip-phen)$^+$ binds firmly into the major groove for the first ∼6 ns. However, after this time, a loss of contact surface between the DNA major groove and the phenanthroline rings occurs (Figure S5B of the Supporting Information), i.e., vdW interactions between DNA and Cu(3-Clip-phen)$^+$ are reduced by about 50%. The hydrogen bond between N−H and O2(T23) keeps the ligand close to the major groove for the rest of the simulation. Possibly, Cu(3-Clip-phen)$^+$ may be fully solvated at longer simulation times.

Thus, after an initial stability of copper complexes/DNA adducts, a progressive solvation of the ligands occurs. These results give a clear rationale for the experimental evidence that DNA cleavage cannot be achieved from the major groove.[10,31]

Cu(phen)$_2^+$: Partial Intercalation. The hypothesis of partial intercalation states that one phenanthroline of Cu(phen)$_2$ lays between two base pairs and the other lies along the minor groove (Figure S2 of the Supporting Information).[31,44,45,52] This is crucially based on the X-ray structure of [Cu(phen)$_2$]$^+$(ClO_4)$^-$, featuring a small dihedral angle of ∼50° between the two

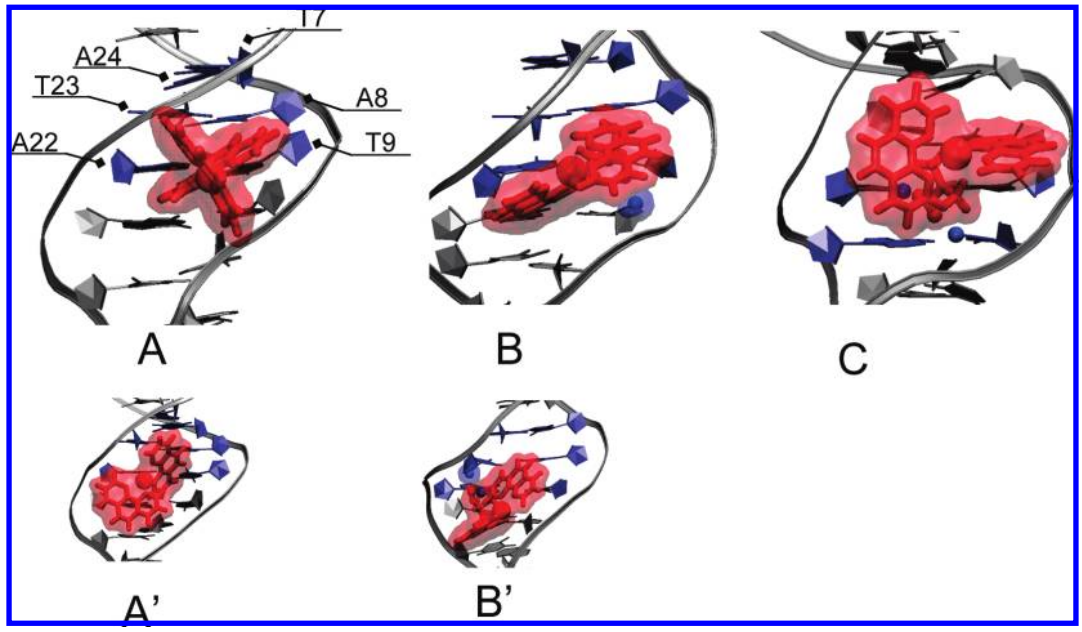

Figure 3. Views of $Cu(phen)_2^+$/DNA (A), $Cu(phen)_2^+{}_B$/DNA (A′), Cu(3-Clip-phen)$^+$/DNA (B), Cu(3-Clip-phen)$^+{}_B$/DNA (B′), and Cu(2-Clip-phen)$^+$/DNA (C). H-bonded atoms are displayed as colored balls.

phenanthroline rings (Table 1). This experimental evidence triggered the hypothesis of partial intercalation of one phen ring inside the DNA.

In order to verify this hypothesis, we first performed DFT optimizations (see the Computational Details section) on geometries of $Cu(phen)_2^+$, Cu(2-Clip-phen)$^+$, and Cu(3-Clip-phen)$^+$ with/without ClO_4^- (for the sake of clarity, data about isolated clipped complexes are discussed in the Supporting Information). We define the energy cost associated with the distortion (strain energy, Table S3 of the Supporting Information) as the difference between the energies of the structure at the minimum and that of the structure obtained from the optimization with ClO_4^-. In line with NMR[54] and theoretical studies,[72,73] our previous DFT calculations had indicated the N1N2N3N4 value to be 81° at the minimum of the potential energy surface of $Cu(phen)_2^+$.[19] DFT calculations in the presence of ClO_4^- give an angle of 58°, confirming a large effect of this counterion on the geometry of the complex. The strain energy associated to this conformation is equal to 13 kcal/mol. However, the energy cost to force N1N2N3N4 to the experimental value of ∼50° is even larger (∼20 kcal/mol). Because of the flexibility of nucleic acids [It is well-known that the DNA minor groove can significantly open to let large ligands inside; see for example refs 28 and 29. In addition, MD simulations showed that the free energy associated to the minor-groove opening is as small as ∼4 kcal/mol for the **TAT**ATA sequence.],[28,29,88,89] it is rather unlikely that DNA can force this ligand to adopt a small dihedral angle and induce partial intercalation. However, one might speculate that intercalation could be allowed by an opening of the DNA bases toward the major groove,[89] rather than by a conformational change of the ligand. To further investigate this possibility, nine steered MD simulations were performed, in which the ligand is initially in front of the **TAT** triplet of the DNA minor groove (see the Computational Details section). Irrespective of the force constants and the velocities employed, the ligand slips along the DNA minor groove and no intercalation is observed.

It is reasonable to assume that these findings are virtually independent of the DNA sequence chosen as related to the structural features of the ligand (e.g., the conformation with a small dihedral angle is not favorable) more than those of the target. Furthermore, partial intercalation is expected to be less likely for clipped complexes mainly because of steric reasons. For instance, the N1N2N3N4 of Cu(2-Clip-phen) is always larger than 70°; Cu(3-Clip-phen) is relatively planar, but the steric hindrance of the link most likely prevents the intercalation.

Our results are thus consistent with previous findings that the N1N2N3N4 angle depends on the environment (i.e., solution or solid state and/or nature of the counterions employed in crystals),[31] thereby supporting the original Sigman's model of minor-groove binding.[31]

Minor-Groove Binding: General Features. The initial configuration of the adducts was obtained via docking of the ligands onto the **TAT** triplet of the 15-mer d(GGCCCT**TAT**-CAGGGC)$_2$. Several poses [One pose for $Cu(phen)_2$/DNA was found. Two poses for Cu(3-Clip-phen)/DNA and two poses for Cu(2-Clip-phen)/DNA were found (with $-NH_2$ pointing inside or outside the DNA).] were used as initial structure for 8 ns MD simulation. By performing a cluster analysis and by monitoring energetic and structural properties, we selected the most relevant representative configurations for each DNA adduct and discussed below (Figure 3). Further details on less relevant configurations are collected in the Supporting Information.

Several properties were employed to characterize the studied DNA adducts:

(A) The N1N2N3N4 dihedral angles were monitored to verify that the small angles observed in some of the X-ray structures (that would allow partial intercalation) are not visited even in the presence of the DNA.

(B) In the case of clipped complexes, the hydrogen bonds between the $-NH_2$ group of the serinol link and DNA bases were analyzed.

(C) Inspired by the finding that Cu···C1′ distances (Figure 2A) may inversely correlate with the probability of RNA cleavage induced by $Cu(phen)_2^+$,[55] distances between sugar carbon atoms and the copper center (Cu···Cn′) were monitored for all the studied copper-complex/DNA adducts (assuming that the behavior observed in RNA adducts may be similar to that of DNA adducts, Figures 4 and S8A, Tables 2 and S4).

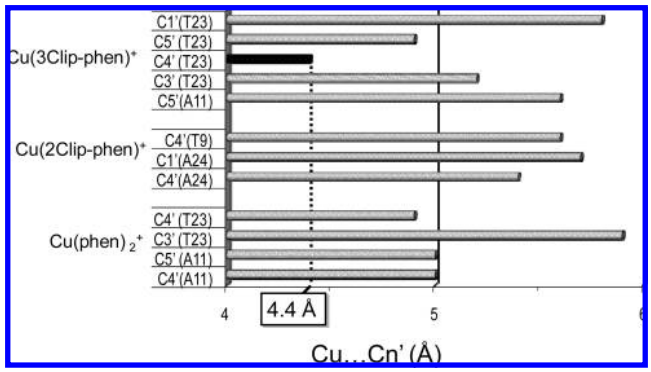

Figure 4. Distribution of Cu···Cn′ distances shorter than 6 Å of most probable copper complexes/DNA adducts.

TABLE 2: Cu···Cn′ Distances for $Cu(phen)_2^+$, $Cu(3\text{-Clip-phen})^+$, and $Cu(2\text{-Clip-phen})^+$/DNA Adducts

	no.[a]	range (Å)[b]	closest base
$Cu(phen)_2^+$	4	4.9−5.9	T23
$Cu(3\text{-Clip-phen})^+$	5	4.4−5.6	T23
$Cu(2\text{-Clip-phen})^+$	3	5.3−5.7	A24

[a] Number of Cu···Cn′ shorter than 6 Å. [b] For further details and standard deviations, see Table S4 in the Supporting Information.

(D) Both van der Waals and electrostatic interactions between ligand and DNA were monitored during the simulations. Since the former is the most relevant source of stabilization in noncovalent ligand/DNA adducts,[82,83] the contribution ($\Delta\Delta E_{vdW}$) to the binding energy was also estimated (Computational Details). A detailed analysis of these energies was carried out to assess (i) which DNA strands interact most strongly with the two phen rings of the ligands (arbitrarily named in Figure 5A as phen1 and phen2) and (ii) which bases have the strongest interactions with the ligands (Figure 5B).

(E) Local and global DNA structural parameters were analyzed. As expected from experimental studies,[10,31] the overall DNA structure hardly changed upon binding, yet intriguing features related to minor-groove width and depth were discussed, that are possibly related to the cleavage efficiency (Figure 6).

$Cu(phen)_2^+$ Adducts. After minimization and molecular dynamics simulation of the initial pose obtained by docking, $Cu(phen)_2^+$ interacts with DNA mostly through nucleobases close to the **TAT** triplet (Figure 3A). A cluster analysis allowed to identify different configurations, the most representative one (found for ∼75% of the time) featuring one phenanthroline ring inside the minor groove, parallel to the minor-groove axis. The second most relevant cluster (Figure 3A′) contains only ∼15% of the ensemble of configurations, with the ligand sitting on the minor-groove edge. For the sake of clarity, the following discussion focuses on the most populated cluster.

No relevant modifications of the N1N2N3N4 dihedral angle were observed, the mean value being ∼80°, with a minimum close to 70° (Figure S6 of the Supporting Information). This further confirms that, even in the presence of DNA, the conformation with N1N2N3N4 ∼50° as found in the X-ray structure of $[Cu(phen)_2^+](ClO_4)^-$ is not likely.[53]

RMSD plots (Figure S7 of the Supporting Information) and particularly the analysis of Cu···Cn′ distances (Table S4, Figures 4 and S8A) suggested that the ligand can adopt several, similar, positions inside the DNA. For instance, both the temporal evolution and the distribution of these distances, confirmed this point (Table S4 and Figure S8A of the Supporting Information showing the trend of Cu···C4′(T23), the shortest distance between the copper center and the sugar backbone in the $Cu(phen)_2^+$/DNA adduct). Interestingly, peaks around 5 ns were observed (Figure S8A). The visual analysis of the MD simulation revealed that at this time the two phen rings swap their positions, with the one inside the groove becoming exposed to the solvent and vice versa.

The analysis of the potential energy indicated that vdW interactions are markedly larger than the electrostatic ones ($\Delta E_{vdW} = -30$ and $\Delta E_{el} = -6$ kcal/mol, Table 3), with T23 and A11 playing a pivotal role for the binding (Figure 5B). Roughly 60% of the overall interaction is localized on these nucleobaes (Figure 5B and Table S5 of the Supporting Information). Dissection of vdW interaction energies confirms that one ring strongly interacts with both DNA strands (about 85% of the overall interaction energy), the other being partially exposed to the solvent, with an interaction energy of −5 kcal/mol (Figure 5A). In addition, the value of the vdW interaction energy between each phen and DNA strands, plotted as a function of time, shows a peak around 5 ns (data not shown), mirroring the behavior discussed above. The van der Waals contribution to the binding energy ($\Delta\Delta E_{vdW}$) was also estimated as mentioned in the Computational Details, this being equal to −4.7 kcal/mol.

Due to the excellent fit of one phenanthroline ring inside the DNA (Figure 6A), the minor-groove width is narrowed from the T7A24 to C10G21 bases (Figure 6B), and its depth increases up to ∼1 Å in the region between T9A22 and C10G21 (Figure 6C).

In summary, MD simulations confirmed that the ligand structure is hardly affected upon binding. $Cu(phen)_2^+$ interacts firmly with the DNA, i.e., one phen tightly fits inside the minor groove, guiding the copper center close to the atoms that undergo the oxidative attack.

$Cu(3\text{-Clip-phen})^+$ Adducts. Adducts obtained by docking $Cu(3\text{-Clip-phen})^+$ to the DNA minor groove resulted in two poses. In the first (termed as $Cu(3\text{-Clip-phen})^+$/DNA), the $-NH_2$ group points inside the DNA, interacting with the strand containing **TAT** nucleobases (Figure 3B). In the second (termed as $Cu(3\text{-Clip-phen})^+_B$/DNA, Figure 3B′), $-NH_2$ points toward the solvent and is closer to the complementary ATA triplet. For each pose, molecular dynamics simulations generated configurations mainly clustered around one single representative. For the sake of clarity, we will focus on the most stable pose (for a brief description of the other pose, see the Supporting Information).

$Cu(3\text{-Clip-phen})^+$ achieves a stable position inside the minor groove after ∼2 ns (see Figures S7 and S8A of the Supporting Information displaying RMSD and time evolution plots of Cu···Cn′, respectively), with one phen ring buried inside the minor groove (in a region spanning from A8 to C10), the other being partially exposed to the solvent. In line with our DFT studies,[19] the covalent bond of the serinol bridge forces the two phenanthroline rings around the minimum N1N2N3N4 value of 50° (Figure S6B of the Supporting Information). Also, the serinol bridge ensures the ligand being anchored to the DNA via two H-bonds, N−H···O4′(C10) and N−H···O2(T9) with average lengths of 2.0 and 2.2 Å, respectively (Table 4 and Figure S8B). In addition, Cu···C4′(T23), the shortest Cu···Cn′ distance of all studied complexes (vide infra) reaches a stable value after ∼2 ns and is virtually constant for the entire simulation time, confirming the stability of the molecule inside the DNA (Figure S8A).

The energetic analysis revealed that vdW interactions between $Cu(3\text{-Clip-phen})^+$ and DNA are the largest of all studied adducts

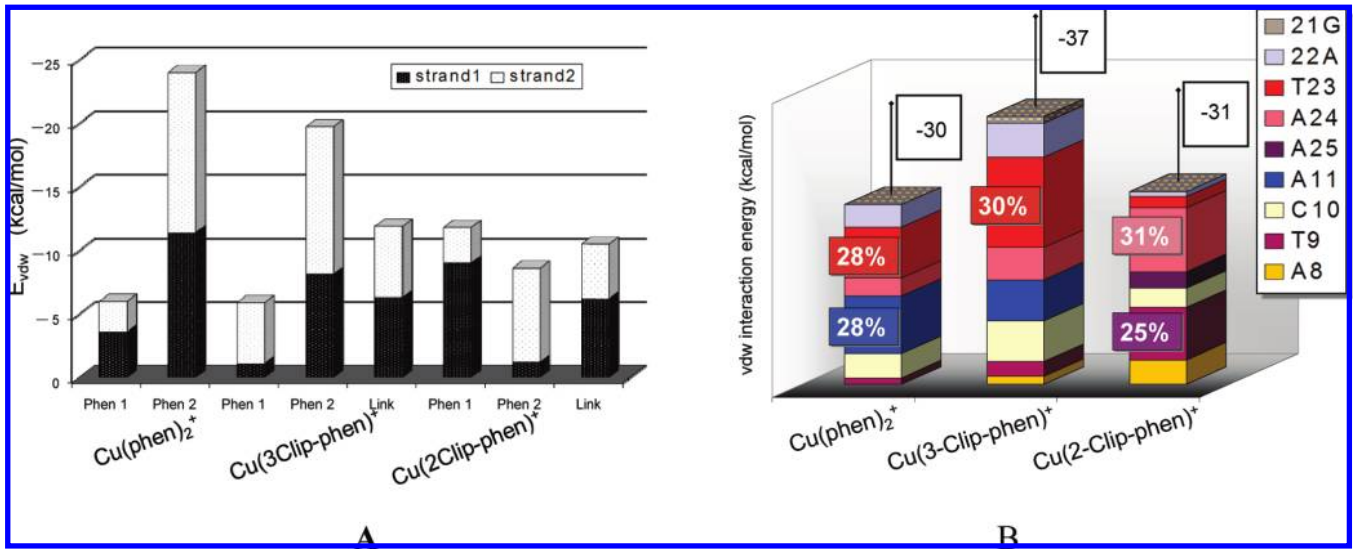

Figure 5. van der Waals interactions partitioned in two different schemes. (A) Contributions from the interaction of the phen rings (arbitrarily named phen1 and phen2) with DNA strands (named strand1 and strand2). (B) Contributions to ΔE_{vdW} from the interaction of the ligand and single DNA nucleobases. ΔE_{vdW} (in the squares in kilocalories per mole) is split into colored cubes whose size is proportional to the strength of the single vdW interaction (kilocalories per mole). For the largest contributions, the percentage to the overall vdW interaction energy is reported. Data in Figure 5B are also displayed in Table S5.

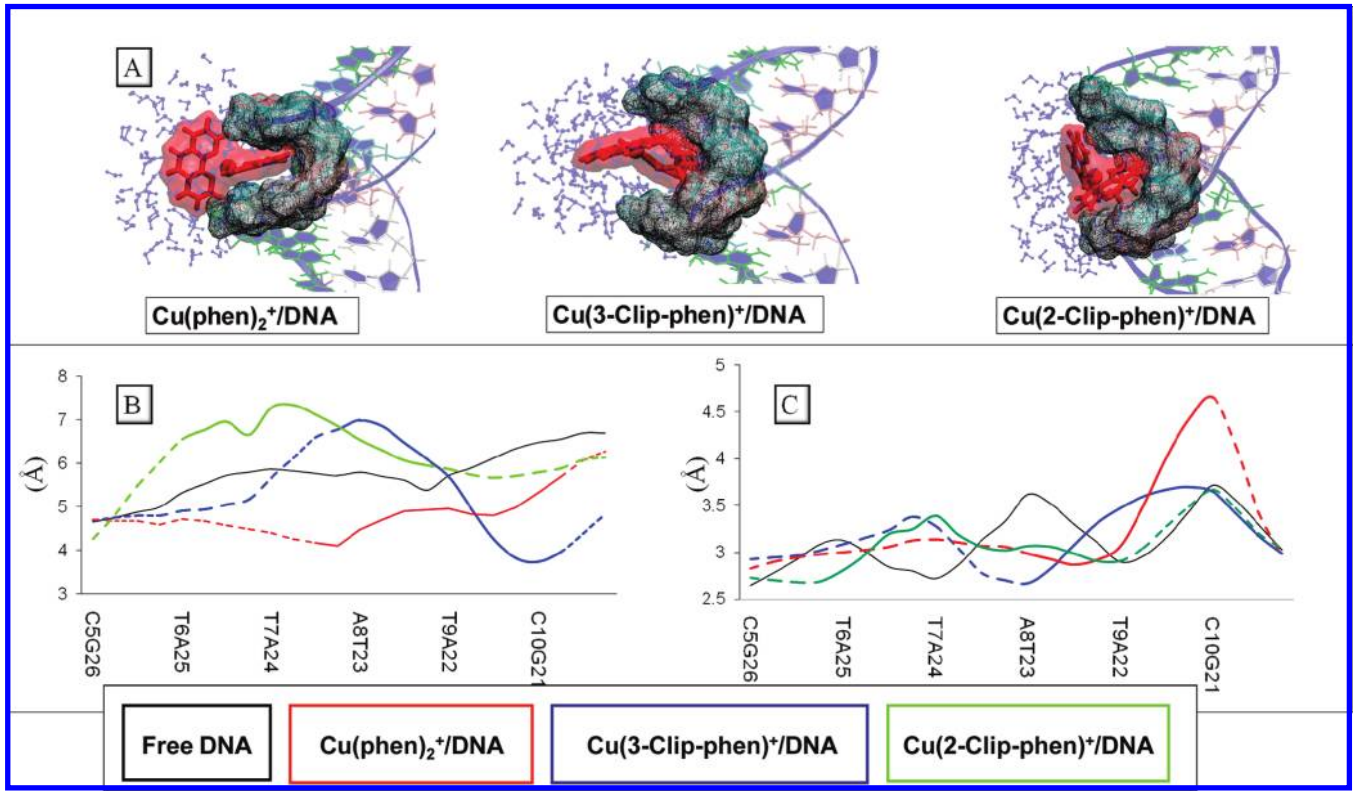

Figure 6. (A) Solvation and minor-groove fit of $Cu(phen)_2^+$, $Cu(3\text{-Clip-phen})^+$, and $Cu(2\text{-Clip-phen})^+$/DNA adducts. (B) Minor-groove width. (C) Minor-groove depth. Continuous lines indicate the binding region.

(vide infra), $\Delta E_{vdW} = -37$ kcal/mol (Table 3). Similarly to $Cu(phen)_2^+$, one phen interacts strongly with both strands ($\Delta E_{vdW} = -20$ kcal/mol, Figure 5A), and the second phen weakly interacts with one strand (with $\Delta E_{vdW} = -5$ kcal/mol). As displayed in Figure 5B (and in Table S5 of the Supporting Information), 30% (−12 kcal/mol) of the overall vdW interaction involves T23, while the remaining 70% is spread over many different bases. An analysis of the electrostatic interactions suggested that the largest contribution is due to the N−H···O4′(C10) and N−H···O2(T9) hydrogen bonds (data not shown). In addition, the van der Waals contribution to the binding energy $\Delta\Delta E_{vdW}$ was also estimated as −11.3 kcal/mol, this being the largest of all studied complexes (vide infra).

The analysis of minor-groove width and depth confirmed that the ligand fits well inside the DNA, as the minor groove narrows in the region covered by the ligand, while adjacent tracts slightly open (Figure 6A). For instance, the minor-groove width decreases by ∼2.5 Å in the base step T9-C10, while from T7 to T9 it increases by ∼1 Å (Figure 6B). The effect of the ligand

TABLE 3: van der Waals and Electrostatic Interaction Energies (ΔE_{vdW} and ΔE_{el}, respectively) of Ligands Binding the Minor Groove[a]

	cleavage efficiency	$\Delta\Delta E_{vdW}$[b]	ΔE_{vdW}	ΔE_{el}
$Cu(phen)_2^+$	1	−4.7	−30 (2)	−6 (2)
$Cu(3\text{-Clip-phen})^+$	60	−11.3	−37 (3)	−11 (2)
$Cu(2\text{-Clip-phen})^+$	2	−6.0	−31 (3)	−14 (3)

[a] Standard deviations are given in brackets. The van der Waals contribution to the binding energy ($\Delta\Delta E_{vdW}$) is also reported. [b] As mentioned in the Computational Details section, the estimation of $\Delta\Delta E_{vdW}$ is very qualitative mainly due to large fluctuations of DNA solvation energies. For this reason, standard deviations were not reported.

TABLE 4: H-Bond Interactions of Copper Complexes DNA Adducts[a]

	no.[Hb,b]	D−H···A	bases	H···A (Å)	DHA (deg)
$Cu(phen)_2^+$					
$Cu(3\text{-Clip-phen})^+$	1.5 (0.6)	N−H···O4′	C10	2.0 (0.2)	162 (11)
		N−H···O2	T9	2.2 (0.4)	137 (18)
$Cu(2\text{-Clip-phen})^+$	1.8 (0.4)	N−H···O2	T23	1.9 (0.2)	163 (9)
		N−H···O2	T9	2.0 (0.2)	149 (14)

[a] Standard deviations are given in brackets. [b] Number of H-bonds averaged over the entire simulation time.

on the minor-groove depth is less evident than that of $Cu(phen)_2^+$ (Figure 6C).

Thus, data obtained about the minor-groove binding of $Cu(3\text{-Clip-phen})^+$ confirmed that the serinol link in C3 provides a clear advantage with respect to $Cu(phen)_2^+$:[10] $Cu(3\text{-Clip-phen})^+$ firmly binds the DNA and the adduct features the strongest vdW interactions of all studied complexes. In addition, due to its favorable geometry, Cu(3-Clip-phen) features the shortest distance between the metal center and C4′(T23) carbon atom.

Cu(2-Clip-phen)$^+$ Adducts. Docking of the ligand to the DNA minor groove produced two different poses, differing by the position of the $-NH_2$ group, which is either pointing inside or outside the minor groove. Only the former is stable for the whole simulation time (Figure 3C), as the latter, characterized by a water exposed $-NH_2$ group, is fully solvated after ∼3 ns (see the Supporting Information for a discussion).

As for $Cu(3\text{-Clip-phen})^+$, MD of the initial pose generated configurations mainly clustered around one single representative. RMSD of $Cu(2\text{-Clip-phen})^+$/DNA indicates that the adduct is fairly stable along the simulation (Figure S7 of the Supporting Information). In addition, the plot of hydrogen bond interactions as a function of time clearly shows that $Cu(2\text{-Clip-phen})^+$ achieves a suitable position inside the minor groove after ∼2 ns (Figure S8 of the Supporting Information), the adduct being stabilized by two N−H···O2(T23 and T9) hydrogen bonds, shorter than those of $Cu(3\text{-Clip-phen})^+$/DNA (Table 4). Upon binding, the dihedral angle between the two phen rings is close to 90°, slightly larger than that of the free ligand calculated via DFT calculations and MD simulations (Table 1, Figure S6C of the Supporting Information).

Electrostatic interactions are stronger than in any other adduct, while vdW interactions between the DNA and the ligand as well as $\Delta\Delta E_{vdW}$ are equivalent to those of $Cu(phen)_2^+$ (Table 3). Despite the intrinsic approximations of a force-field based MD scheme, a qualitative correlation between vdW interaction energies and the cleavage efficiency exists, Cu(3-Clip-phen) > Cu(2-Clip-phen) > $Cu(phen)_2$. [Further calculations and/or experiments are required to prove beyond doubt that vdW interactions between these compounds and DNA can effectively modulate the cleavage efficiency. Besides the approximations of the employed methods, the interaction of copper(I) complexes is only the first step of a very complex redox reaction (see the Introduction section).] As it may be expected, the van der Waals contribution to binding energy ($\Delta\Delta E_{vdW}$) shows the same qualitative trend as ΔE_{vdW}.[82,83]

Further energetic analysis revealed that the interaction between $Cu(2\text{-Clip-phen})^+$ and DNA is rather different compared to the other two complexes. For instance, each aromatic ring interacts with one strand only, i.e., the ligand sits on the edge of the minor groove (Figures 5 and 6A). In line with this finding, Cu···Cn′ distances, albeit stable during the simulation time, are longer by ∼1 Å than those of $Cu(3\text{-Clip-phen})^+$ and $Cu(phen)_2^+$/DNA adducts (Tables 2 and S4, Figures 4 and S8A). In addition, unlike the other ligands, $Cu(2\text{-Clip-phen})^+$ induces a broad minor-groove opening, from T6 to T9, with a maximum increase of ∼2 Å with respect to free DNA (Figure 6B). Consistent with these data is the fact that the minor-groove depth is virtually unchanged upon binding, leading to the conclusion that the ligand cannot penetrate the DNA (Figure 6C).

In summary, structural and energetic data revealed three important aspects: (i) vdW interactions between $Cu(2\text{-Clip-phen})^+$ and DNA are equivalent to those of $Cu(phen)_2^+$/DNA and weaker than those of $Cu(3\text{-Clip-phen})^+$/DNA; (ii) N−H···O H-bonds are more stable than those of the $Cu(3\text{-Clip-phen})^+$/DNA adduct; (iii) the DNA minor groove markedly opens upon binding. Thus, besides the increased affinity of copper for the second phenanthroline ring, the main advantage of clipping the phenanthroline rings via the serinol link on C2 atoms is due to the possibility of forming hydrogen bonds. However, $Cu(2\text{-Clip-phen})^+$ keeps a very large N1N2N3N4 dihedral angle for the entire simulation and the DNA minor groove has to open to accommodate such a bulky ligand. This leads to an increased distance between the metal center and the atoms that undergo cleavage. This finding may be one of the key factors for the different DNA cleavage efficiency of Cu(2-Clip-phen) and Cu(3-Clip-phen) complexes.

Efficiency of Copper−1,10-Phenanthroline Complexes. As mentioned in the introduction, the main reason of the enhanced cleavage efficiency of clipped complexes with respect to $Cu(phen)_2$ is the increased affinity for the second phen ring.[10,31] The large enhancement in the cleavage activity observed for Cu(3-Clip-phen) with respect to Cu(2-Clip-phen) is, however, still poorly understood.[10,19]

Knowing the exact nature of the active species is crucial to study the different reactivity of $Cu(phen)_2$, Cu(3-Clip-phen), and Cu(2-Clip-phen) complexes. However, neither experimental nor theoretical studies have been able to conclusively prove which transient species are formed during the radical reactions leading to DNA cleavage.[10] The scenario is indeed very intricate, as several factors (such as the structural properties of the ligand, energetic barrier of radical reactions, DNA rearrangements upon reaction, etc.) may contribute to the reactivity of these complexes. Nevertheless, it has been suggested that the position of copper(I)−phenanthroline complexes inside the minor groove may be related to the cleavage efficiency of RNA nucleobases.[55] Assuming that this behavior is preserved for DNA adducts, we monitored all the distances between the metal center and the DNA sugar carbon atoms to possibly relate cleavage efficiency of each ligand to the position inside the minor groove (Tables 2 and S4, Figures 4 and S8A).

In particular, distances between copper and sugar carbon atoms in $Cu(phen)^+$/DNA and $Cu(3\text{-Clip-phen})^+$/DNA adducts

range between 4.4 and 5.9 Å (Tables 2 and S4, Figures 4 and S8A). Cu···Cn′ distances in Cu(2-Clip-phen)$^+$/DNA adducts are typically longer by 1 Å, ranging between 5.4 and 5.7 Å (Figure 4). Perhaps the most important finding is that the shortest Cu···Cn′ distance of all studied adducts is observed in the adducts containing Cu(3-Clip-phen).

These data suggest that Cu(3-Clip-phen) may be a more efficient cleaver than Cu(2-Clip-phen) as the metal center is closer to the sugar carbon atoms. In contrast, the potential cleavage efficiency of Cu(2-Clip-phen) is hampered by the unfavorable position inside the groove, i.e., the copper center lies at larger distances from the atoms to be cleaved. In line with our previous studies based on DFT calculations,[19] we suggest that the only reason of the cleavage improvement by use of Cu(2-Clip-phen) to be the increased affinity for the second phen. Besides this, Cu(3-Clip-phen) ensures a good fit inside the minor groove and a better interaction with DNA.

Interestingly, it has been suggested that also protonation of the amino groups of the clipped complexes may influence reactivity.[15] Moreover, it cannot be a priori excluded that upon oxidation this scenario might alter because of a conformational change of the copper coordination sphere, the formation of reactive species, or subsequent rearrangements of DNA. Yet, our recent DFT studies have shown that the oxidation state of Clip-phen complexes (and formation of five-coordinated species) mainly affects Cu−N bonds, with no other major modifications occurring to the geometry of the ligand.[19] Furthermore, structural rearrangements of DNA might require longer times than those needed for the radical reactions that lead to cleavage. Although more experimental and computational studies are required to investigate all factors that can influence the cleavage efficiency of these important compounds, this investigation provides a first insight into the relationship between reactivity and structural properties.

Conclusions

In this work, a combination of techniques such as DFT, molecular docking, and classical molecular dynamics simulations was employed to explore the noncovalent DNA binding modes of copper−1,10-phenanthroline complexes, as the first step toward cleavage of DNA. The clipped complexes were modeled with neutral amino groups which allows us to compare these results with our previous studies.[19,56]

First, a rationale was given to explain the experimental evidence that Cu(phen)$_2$, Cu(2-Clip-phen), and Cu(3-Clip-phen) cannot cleave from the major groove:[10] none of the studied complexes was stable in this position as a progressive solvation of the ligands occurs.

Second, the partial intercalation hypothesis of Cu(phen)$_2^+$/DNA adducts previously proposed was investigated:[31,45] our steered MD simulations showed that Cu(phen)$_2$ preferentially interacts with the DNA minor groove. For the first time, a systematic theoretical work, based on a combination of classical and quantum techniques, fully supports the experimental model of minor-groove binding.[31]

In addition, our results strongly suggest that cleavage may be directly related to structural properties. The analysis of the minor-groove width revealed that both Cu(phen)$_2$ and Cu(3-Clip-phen) narrow the minor groove in the binding region, while the bulkier Cu(2-Clip-phen) opens the minor groove in a region spanning several nucleobases. This scenario is mirrored by the distances between the copper metal center and the sugar carbon atoms, which may inversely correlate with the cleavage efficiency.[55] In particular, Cu(3-Clip-phen) complexes showed the shortest Cu···Cn′ distances among all studied ligand/DNA adducts.

In conclusion, our results clearly suggest that the better minor-groove fit (Figure 6) of Cu(3-Clip-phen) may contribute to the enhanced cleavage activity with respect to Cu(2-Clip-phen). 3-Clip-phen ligands impose a more planar geometry to the copper complex favoring the fit inside the minor groove, in turn allowing the metal to lie at shorter distances from the atoms that undergo the oxidative attack. In contrast, Cu(2-Clip-phen) sits at the edge of the minor groove and causes severe distortion of the minor groove, resulting in a lower cleavage efficiency. In line with previous studies,[55] our results confirm that the position of the metal center inside the minor groove may be one of the key factors of the cleavage efficiency of copper−1,10-phenanthroline complexes.

Acknowledgment. Computational resources were granted by CINECA (INFM grant) and CASPUR (SLACS collaboration). This work was carried out in the frame of the project "New Antitumoral Technologies" (Art. 11 L.R. 11/2003, Art. 7 del "Regolamento per la concessione di contributi per la realizzazione di progetti di ricerca scientifica e applicata e di iniziative di trasferimento e di diffusione dei risultati della ricerca"). This work makes use of results produced by the Cybersar Project managed by the Consorzio COSMOLAB, a project cofunded by the Italian Ministry of University and Research (MIUR) within the Programma Operativo Nazionale 2000−2006 "Ricerca Scientifica, Sviluppo Tecnologico, Alta Formazione per le Regioni Italiane dell'Obiettivo 1 (Campania, Calabria, Puglia, Basilicata, Sicilia, Sardegna) Asse II, Misura II.2 Società dell'Informazione, Azione a Sistemi di calcolo e simulazione ad alte prestazioni". More information is available at http://www.cybersar.it. The authors are indebted to CERC3 and the Chemical Research Council of The Netherlands, grant number 700_52_705, for financial support.

Supporting Information Available: Steering dynamics, test calculations; effects of counterions on clipped complexes; MD of Cu(3-Clip-phen)^+_B/DNA and Cu(2-Clip-phen)^+_B/DNA; Tables S1−S5; Figures S1−S8; zip file containing the entire force field set of copper−1,10-phenanthroline complexes; MovieS1 showing the intercalation of daunomycin inside the DNA. This material is available free of charge via the Internet at http://pubs.acs.org.

References and Notes

(1) Burda, J. V.; Zeizinger, M.; Leszczynski, J. *J. Comput. Chem.* **2005**, *26*, 907–914.
(2) Jamieson, E. R.; Lippard, S. J. *Chem. Rev.* **1999**, *99*, 2467–2498.
(3) Kozelka, J.; Legendre, F.; Reeder, F.; Chottard, J. C. *Coord. Chem. Rev.* **1999**, *192*, 61–82.
(4) Alessio, E.; Mestroni, G.; Bergamo, A.; Sava, G. *Met. Ions Biol. Syst.* **2004**, *42*, 323–351.
(5) Alessio, E.; Mestroni, G.; Bergamo, A.; Sava, G. *Curr. Top. Med. Chem.* **2004**, *4*, 1525–1535.
(6) Chabner, B. A.; Roberts, T. G. *Nat. Rev. Cancer* **2005**, *5*, 65–72.
(7) Hurley, L. H. *Nat. Rev. Cancer* **2002**, *2*, 188–200.
(8) van Zutphen, S.; Reedijk, J. *Coord. Chem. Rev.* **2005**, *249*, 2845–2853.
(9) de Hoog, P.; Boldron, C.; Gamez, P.; Sliedregt-Bol, K.; Roland, I.; Pitie, M.; Kiss, R.; Meunier, B.; Reedijk, J. *J. Med. Chem.* **2007**, *50*, 3148–3152.
(10) Pitié, M.; Boldron, C.; Pratviel, G. *Adv. Inorg. Chem.* **2006**, *58*, 77–130.
(11) Jiang, Q.; Xiao, N.; Shi, P.; Zhu, Y.; Guo, Z. *Coord. Chem. Rev.* **2007**, *251*, 1951–1972.
(12) Sigman, D. S.; Graham, D. R.; Daurora, V.; Stern, A. M. *J. Biol. Chem.* **1979**, *254*, 2269–2272.

(13) Deegan, C.; McCann, M.; Devereux, M.; Coyle, B.; Egan, D. A. *Cancer Lett.* **2007**, *247*, 224–233.
(14) Pitié, M.; Sudres, B.; Meunier, B. *Chem. Commun.* **1998**, 2597–2598.
(15) Pitié, M.; Boldron, C.; Gornitzka, H.; Hemmert, C.; Donnadieu, B.; Meunier, B. *Eur. J. Inorg. Chem.* **2003**, 528–540.
(16) Veal, J. M.; Rill, R. L. *Biochemistry* **1988**, *27*, 1822–1827.
(17) Veal, J. M.; Rill, R. L. *Biochemistry* **1989**, *28*, 3243–3250.
(18) Pitié, M.; Donnadieu, B.; Meunier, B. *Inorg. Chem.* **1998**, *37*, 3486–3489.
(19) Robertazzi, A.; Magistrato, A.; deHoog, P.; Carloni, P.; Reedijk, J. *Inorg. Chem.* **2007**, *46*, 5873–5881.
(20) Pitié, M.; Van Horn, J. D.; Brion, D.; Burrows, C. J.; Meunier, B. *Bioconjugate Chem.* **2000**, *11*, 892–900.
(21) Pitié, M.; Burrows, C. J.; Meunier, B. *Nucleic Acids Res.* **2000**, *28*, 4856–4864.
(22) Bales, B. C.; Kodama, T.; Weledji, Y. N.; Pitie, M.; Meunier, B.; Greenberg, M. M. *Nucleic Acids Res.* **2005**, *33*, 5371–5379.
(23) Pitié, M.; Meunier, B. *Bioconjugate Chem.* **1998**, *9*, 604–611.
(24) Spiegel, K.; Magistrato, A.; Carloni, P.; Reedijk, J.; Klein, M. L. *J. Phys. Chem. B* **2007**, *111*, 11873–11876.
(25) Robertazzi, A.; Platts, J. A. *Chem.—Eur. J.* **2006**, *12*, 5747–5756.
(26) Lauria, A.; Montalbano, A.; Barraja, P.; Dattolo, G.; Almerico, A. M. *Curr. Med. Chem.* **2007**, *14*, 2136–2160.
(27) Dolenc, J.; Baron, R.; Oostenbrink, C.; Koller, J.; van Gunsteren, W. F. *Biophys. J.* **2006**, *91*, 1460–1470.
(28) Baraldi, P. G.; Preti, D.; Fruttarolo, F.; Tabrizi, M. A.; Romagnoli, R. *Bioorg. Med. Chem.* **2007**, *15*, 17–35.
(29) Dyke, M. W. V.; Hertzberg, R. P.; Dervan, P. B. *Proc. Natl. Acad. Sci.* **1982**, *79*, 5470–5474.
(30) Vargiu, A. V.; Ruggerone, P.; Magistrato, A.; Carloni, P. *Nucleic Acids Res.* **2008**, *36*, 5910–5921.
(31) Sigman, D. S.; Mazumder, A.; Perrin, D. M. *Chem. Rev.* **1993**, *93*, 2295–2316.
(32) Meijler, M. M.; Zelenko, O.; Sigman, D. S. *J. Am. Chem. Soc.* **1997**, *119*, 1135–1136.
(33) Oyoshi, T.; Sugiyama, H. *J. Am. Chem. Soc.* **2000**, *122*, 6313–6314.
(34) Goyne, T. E.; Sigman, D. S. *J. Am. Chem. Soc.* **1987**, *109*, 2846–2848.
(35) Kuwabara, M.; Yoon, C.; Goyne, T.; Thederahn, T.; Sigman, D. S. *Biochemistry* **1986**, *25*, 7401–7408.
(36) Chen, T.; Greenberg, M. M. *J. Am. Chem. Soc.* **1998**, *120*, 3815–3816.
(37) Kalsani, V.; Schmittel, M.; Listorti, A.; Accorsi, G.; Armaroli, N. *Inorg. Chem.* **2006**, *45*, 2061–2067.
(38) Miller, M. T.; Gantzel, P. K.; Karpishin, T. B. *Inorg. Chem.* **1998**, *37*, 2285–2290.
(39) Hirohama, T.; Kuranuki, Y.; Ebina, E.; Sugizaki, T.; Arii, H.; Chikira, M.; Tamil Selvi, P.; Palaniandavar, M. *J. Inorg. Biochem.* **2005**, *99*, 1205–1219.
(40) Sigman, D. S. *Acc. Chem. Res.* **1986**, *19*, 180–186.
(41) Pratviel, G.; Bernadou, J.; Meunier, B. *Angew. Chem., Int. Ed.* **1995**, *34*, 746–769.
(42) Pogozelski, W. K.; Tullius, T. D. *Chem. Rev.* **1998**, *98*, 1089–1107.
(43) Chen, C. H. B.; Milne, L.; Landgraf, R.; Perrin, D. M.; Sigman, D. S. *Chembiochem* **2001**, *2*, 735–740.
(44) Veal, J. M.; Rill, R. L. *Biochemistry* **1991**, *30*, 1132–1140.
(45) Stockert, J. C. *J. Theor. Biol.* **1989**, *137*, 107–111.
(46) Drew, H. R. *J. Mol. Biol.* **1984**, *176*, 535–537.
(47) Goldstein, S.; Czapski, G. *J. Am. Chem. Soc.* **1986**, *108*, 2244–2250.
(48) Uesugi, S.; Shida, T.; Ikehara, M.; Kobayashi, Y.; Kyogoku, Y. *J. Am. Chem. Soc.* **1982**, *104*, 5494–5495.
(49) Marshall, L. E.; Graham, D. R.; Reich, K. A.; Sigman, D. S. *Biochemistry* **1981**, *20*, 244–250.
(50) Que, B. G.; Downey, K. M.; So, A. G. *Biochemistry* **1980**, *19*, 5987–5991.
(51) Drew, H. R.; Travers, A. A. *Cell* **1984**, *37*, 491–502.
(52) Veal, J. M.; Merchant, K.; Rill, R. L. *Nucleic Acids Res.* **1991**, *19*, 3383–3388.
(53) Healy, P. C.; Engelhardt, L. M.; Patrick, V. A.; White, A. H. *J. Chem. Soc., Dalton Trans.* **1985**, 2541–2545.
(54) Ruthkosky, M.; Castellano, F. N.; Meyer, G. J. *Inorg. Chem.* **1996**, *35*, 6406–6412.
(55) Hermann, T.; Heumann, H. *RNA* **1995**, *1*, 1009–1017.
(56) de Hoog, P.; Louwerse, M. J.; Gamez, P.; Pitié, M.; Baerends, E. J.; Meunier, B.; Reedijk, J. *Eur. J. Inorg. Chem.* **2008**, *2008*, 612–619.
(57) Wang, J.; Wang, W.; Kollman, P. A.; Case, D. A. *J. Mol. Graphics Modell.* **2006**, *25*, 247–260.
(58) Garrett, M. M.; David, S. G.; Robert, S., H.; Ruth Huey, W. E.; Hart, R.; K.; Belew Arthur, J., O. *J. Comput. Chem.* **1998**, *19*, 1639–1662.
(59) Evans, D.; Neidle, S. *Indian J. Med. Chem.* **2006**, *49*.
(60) Frisch, M. J.; Trucks, G. W.; Schlegel, H. B.; Scuseria, G. E.; Robb, M. A.; Cheeseman, J. R.; Montgomery J. A., Jr.; Vreven, T.; Kudin, K. N.; Burant, J. C.; Millam, J. M.; Iyengar, S. S.; Tomasi, J.; Barone, V.; Mennucci, B.; Cossi, M.; Scalmani, G.; Rega, N.; Petersson, G. A.; Nakatsuji, H.; Hada, M.; Ehara, M.; Toyota, K.; Fukuda, R.; Hasegawa, J.; Ishida, M.; Nakajima, T.; Honda, Y.; Kitao, O.; Nakai, H.; Klene, M.; Li, X.; Knox, J. E.; Hratchian, H. P.; Cross, J. B.; Bakken, V.; Adamo, C.; Jaramillo, J.; Gomperts, R.; Stratmann, R. E.; Yazyev, O.; Austin, A. J.; Cammi, R.; Pomelli, C.; Ochterski, J. W.; Ayala, P. Y.; Morokuma, K.; Voth, G. A.; Salvador, P.; Dannenberg, J. J.; Zakrzewski, V. G.; Dapprich, S.; Daniels, A. D.; Strain, M. C.; Farkas, O.; Malick, D. K.; Rabuck, A. D.; Raghavachari, K.; Foresman, J. B.; Ortiz, J. V.; Cui, Q.; Baboul, A. G.; Clifford, S.; Cioslowski, J.; Stefanov, B. B.; Liu, G.; Liashenko, A.; Piskorz, P.; Komaromi, I.; Martin, R. L.; Fox, D. J.; Keith, T.; Al Laham, M. A.; Peng, C. Y.; Nanayakkara, A.; Challacombe, M.; Gill, P. M. W.; Johnson, B.; Chen, W.; Wong, M. W.; Gonzalez, C.; Pople, J. A. *Gaussian03,* Gaussian, Inc.; Wallingford, CT, 2004.
(61) Becke, A. D. *Phys. Rev. A* **1988**, 3098.
(62) Andrae, D.; Haussermann, U.; Dolg, M.; Stoll, H.; Preuss, H. *Theor. Chim. Acta* **1990**, *77*, 123–141.
(63) Cammi, R.; Mennucci, B.; Tomasi, J. *J. Phys. Chem. A* **2000**, 9100.
(64) Pearlman, D. A.; Case, D. A.; Caldwell, J. W.; Ross, W. R.; Cheatham, T. E., III; DeBolt, S.; Ferguson, D.; Seibel, G.; Kollman, P. *Comput. Phys. Commun.* **1995**, *91*, 1–41.
(65) Jorgensen, W. L.; Chandrasekhar, J.; Madura, J. D.; Impey, R. W.; Klein, M. L. *J. Chem. Phys.* **1983**, *79*, 926–935.
(66) Aqvist, J. *J. Phys. Chem.* **1990**, *95*, 8021–8024.
(67) Wang, J.; Wolf, R. M.; Caldwell, J. W.; Kollman, P. A. *J. Comput. Chem.* **2004**, *25*, 1157–1174.
(68) Besler, B. H.; Merz, K. M.; Kollman, P. A. *J. Comput. Chem.* **1990**, *11*, 431–439.
(69) Bayly, C. I.; Cieplak, P.; Cornell, W.; Kollman, P. A. *J. Phys. Chem.* **1993**, *97*, 10269–10280.
(70) Lybrand, T. P.; Creighton, S.; Shafer, R. H.; Kollman, P. A. *J. Mol. Biol.* **1986**, *191*, 495–507.
(71) King, G.; Gembicky, M.; Coppens, P. *Acta Crystallogr., Sect. C: Cryst. Struct. Commun.* **2005**, *61*, M329−M332.
(72) Chen, L. X.; Shaw, G. B.; Novozhilova, I.; Liu, T.; Jennings, G.; Attenkofer, K.; Meyer, G. J.; Coppens, P. *J. Am. Chem. Soc.* **2003**, *125*, 7022–7034.
(73) Zgierski, M. Z. *J. Chem. Phys.* **2003**, *118*, 4045–4051.
(74) Darden, T.; York, D.; Pedersen, L. *J. Chem. Phys.* **1993**, *98*, 10089–10092.
(75) Nosé, S. *Mol. Phys.* **1984**, *52*, 255–268.
(76) Hoover, W. G. *Phys. Rev. A* **1985**, *31*, 1695–1697.
(77) Parrinello, M.; Rahman, A. *J. Appl. Phys.* **1981**, *52*, 7182–7190.
(78) Hess, B.; Bekker, H.; Berendsen, H. J. C.; Fraaije, J. G. E. M. *J. Comput. Chem.* **1997**, *18*, 1463–1472.
(79) Izrailev, S.; Stepaniants, S.; Isralewitz, B.; Kosztin, D.; Lu, H.; Molnar, F.; Wriggers, W.; Schulten, K. *Computational Molecular Dynamics: Challenges, Methods, Ideas*; Springer-Verlag: Berlin, 1998; Vol. 4.
(80) Isralewitz, B.; Gao, M.; Schulten, K. *Curr. Opin. Struct. Biol.* **2001**, *11*, 224.
(81) Swaminatha, S.; Ravishanker, G.; Beveridge, D. L.; Lavery, R.; Etchebest, C.; Sklenar, H. *J. Mol. Model.* **1990**, *8*, 179–193.
(82) Shieh, H. S.; Berman, H. M.; Dabrow, M.; Neidle, S. *Nucleic Acids Res.* **1980**, *8*, 85–97.
(83) Zhou, Z.; Madrid, M.; Evanseck, J. D.; Madura, J. D. *J. Am. Chem. Soc.* **2005**, *127*, 17253–17260.
(84) Daura, X.; Gademann, K.; Seebach, B. J. D.; van Gunsteren, W. F.; Mark, A. E. *Angew. Chem., Int. Ed.* **1999**, *38*, 236–240.
(85) van der Spoel, D.; van Drunen, R.; Berendsen, H. J. C. *GROningen MAchine for Chemical Simulation*: Department of Biophysical Chemistry, BIOSON Research Institute: Nijenborgh 4 NL-9717 AG Groningen, 1994.
(86) van Gunsteren, W. F.; Billeter, S. R.; Eising, A. A.; Hunenberger, P. H.; Kruger, P.; Mark, A. E.; Scott, W. R. P.; Tironi, I. G. *Biomolecular simulation: the GROMOS96 manual and user guide*; Hochschulverlag AG an der ETH: Zurich, 1996.
(87) Berendsen, H. J. C.; Vanderspoel, D.; Vandrunen, R. *Comput. Phys. Commun.* **1995**, *91*, 43–56.
(88) Zacharias, M. *Biophys. J.* **2006**, *91*, 882–891.
(89) Giudice, E.; Varnai, P.; Lavery, R. *Nucleic Acids Res.* **2003**, *31*, 1434–1443.

JP901210G